

Contribution of Gas and Electric Stoves to Residential Ultrafine Particle Concentrations between 2 nm and 64 nm: Size Distributions and Emission and Coagulation Rates

Supporting Information

Lance Wallace*, Fang Wang, Cynthia Howard-Reed, Andrew Persily

Lance Wallace
11568 Woodhollow Court
Reston VA 20191
llwallace73@comcast.net
703-620-4543

Andrew Persily, Cynthia Howard-Reed, and Fang Wang
National Institute of Standards and Technology
100 Bureau Drive MS8633
Gaithersburg, MD 20899

Number of pages: 17

Number of tables: 5

Number of figures: 6

SMPS

Flow rates on the SMPS were measured every few days while the data were being downloaded. The aerosol intake flow (nominally 0.025 L/s) was measured in triplicate and the results were required to be within 2 % precision before beginning any experiment.

A false background counting rate of < 0.01 particle per cm^3 over a 1 h averaging period is stated by the manufacturer (17). Our averaging period is on the order of 1 s, and therefore the false counts were occasionally a serious problem, particularly when multiplied by a large diffusion error coefficient. This made it necessary to manually remove obvious false counts from the files. If a count was observed that was surrounded by counts of zero in all neighboring size categories, it was considered anomalous and removed. These corrections affected $\approx 0.15\%$ of the total measurements. Background levels of UFP typically varied from 100 cm^{-3} to 1000 cm^{-3} , and were negligible compared to maximum concentrations due to cooking.

Some experiments cooking food on the gas stove were affected by a wick in the CPC that was used beyond its lifetime. This resulted in decreased sensitivity to the smallest particles, but had no effect on particles $> 10 \text{ nm}$. All reported results for particles $< 10 \text{ nm}$ were obtained with a fresh wick. The results for particles $> 10 \text{ nm}$ include all experiments.

The detection efficiency of the water-based CPC depends partly on the composition of the particles, with water-soluble particles the most easily detected. Using somewhat greater temperature differences than the recommended values, Mordas et al (18) found 50 % detection efficiency diameters of 1.8 nm for sodium chloride and 2.3 nm for ammonium sulfate. At the default operating temperature of the Model 3786, these diameters would increase somewhat. However, for insoluble or oily particles, the 50% detection efficiency has been found to be near 4 nm or 5 nm (17, 18).

Second CPC

A second instrument was used to measure spatial variability in the home and to compare with the SMPS. This instrument is a portable CPC with isopropyl alcohol as the working fluid (Model 3007, TSI). The concentration uncertainty is stated by the manufacturer to be 20 %. The Model 3007 has a lower cutoff of 10 nm and an upper cutoff of about $1 \mu\text{m}$, so the comparison was with the SMPS sum of particles $> 10 \text{ nm}$. For these experiments the vast majority of particles were smaller than 64 nm, so the difference in the upper cutoffs of the two instruments is of little moment. The two instruments agreed well at low concentrations, but at higher concentrations ($50\,000 \text{ cm}^{-3}$ to $100\,000 \text{ cm}^{-3}$) the SMPS estimates often exceeded those by the Model 3007, by amounts on the order of 20 %. The Model 3007 is expected to underestimate high concentrations (near $100,000 \text{ cm}^{-3}$) due to particle coincidence in the sensing chamber.

Air Change Rates

In each room, the tracer gas concentration was measured every 10 min. The GC/ECD was calibrated every few weeks for a concentration range of 0.018 mg/m^3 to 1.8 mg/m^3 (18 point

calibration) with an uncertainty of about $\pm 5\%$ of the reading. The time until good mixing was achieved (defined as relative standard deviation $<10\%$ across six rooms) was typically 40-50 minutes following injection of the SF₆. After this time, air change rates were calculated by regressing the natural logarithm of the tracer gas concentration versus time according to ASTM method E741(20). The air change rate associated with a given time is based on the three measurements preceding and following that time, so each regression represents a 70 min average air change rate. The air change rate measurements were calculated independently for each of six rooms in the house: kitchen, dining room, living room, family room, master bedroom, and bedroom 2 (Figure S1). The relative standard deviations (RSD) across the rooms were less than 10% (median value of 9%) in 11 099 of the 15 350 calculated air change rates, indicating good mixing across all rooms.

Uncertainties

Limitations of the study include uncertainties in both measurement and models. Although the SMPS classifier is considered a reference instrument for particle size, the number concentrations are subject to error. The manufacturer lists the uncertainty of the water-based CPC (Model 3786) as 12% (17). However, this uncertainty would be increased by low number counting errors, such as would occur for the tails of the distributions (27). The efficiency of the water-based CPC at the smallest sizes (2 nm to 4 nm) is dependent on the composition of the particles (better for hygroscopic and worse for hydrophobic particles). No correction was made for detection efficiency since the composition is unknown; therefore the concentrations for this size range are underestimated. There are very large losses due to diffusion for these small particles; although corrections have been applied, the correction factors are large and the numbers often small, so random variation would be expected to be an important source of error. The flow rates were periodically measured in triplicate and required to show a precision of 2%. For the best cases (large number concentrations and particle diameters > 4 nm), the minimum measurement error associated with a particular particle size category would be the sum (in quadrature) of the errors associated with particle size (1%), number (12%), and flow rate (2%), or slightly more than 12%. For the worst cases (low number concentration, hydrophobic particles, diameters < 4 nm), the measurement error would be larger. When calculating total number concentrations, the relative error is substantially reduced, since the total is summed across 97 size categories. This comment also holds for the calculation of emission rates, since the total error consists of the reduced error associated with the sum across all size categories as well as the small errors in the measurement of cooking time and house volume.

Uncertainties in the models include the assumption of instantaneous perfect mixing in the calculation of emission rates. The maximum total concentration was usually achieved in the master bedroom within the first or second scan (2.5 min or 5 min after the source was turned off). For the coagulation models, we lack knowledge of the composition of the particles, which affects the choice of the Hamaker constant. The shape of the particles is also largely unknown, as is the fraction of particles that are aggregates and may have a fractal dimension. The magnitude of the fractal dimension and the proportion of particles to which it applies are also unknown. The calculated collision kernels (with the Fuchs correction) for the six possible

pairwise collisions of 2 nm, 10 nm, and 100 nm particles were compared to a reference table (21) and found to range within 0 % to 2.5 % of the values supplied.

Coagulation calculation algorithm

Coagulation occurs when particles strike each other and join to form a single larger particle. The probability of collision is a function of the number densities N_i of each particle, their diameters d_i , and their associated diffusion coefficients D_i .

Coagulation rates vary according to how the diameter of the particles compares to the mean free path of the fluid in which they are immersed. The ratio of the two is the Knudsen number:

$$Kn = \frac{\lambda}{r}$$

where r is the radius of the particle.

The mean free path of an air molecule at 300 K is approximately 64 nm. Because our diameters range from 2 nm to 64 nm, Kn also happens to range from 2 to 64. Therefore the smallest particles are in the free-molecular regime ($Kn > 10$), and the larger ones are in the transition regime. Since the equations for coagulation rates vary by regime, it is necessary to develop an adjusted coagulation equation that will work for both regimes.

The rate of collision between any two particle sizes i and j is determined by K_{ij} where

$$K_{ij} = 2\pi(d_i + d_j)(D_i + D_j)\beta_{ij}$$

where d is the diameter of the particle and D is its Brownian diffusion coefficient.

β_{ij} is the dimensionless Fuchs coefficient providing for the transition between regimes, given by

$$\left(\frac{d_i + d_j}{d_i + d_j + 2(g_i^2 + g_j^2)^{0.5}} + \frac{8(D_i + D_j)}{(c_i^2 + c_j^2)^{0.5}(d_i + d_j)} \right)^{-1}$$

where

$$c_i = \left(\frac{8kT}{\pi m_i} \right)^{0.5}$$

$$l_i = \frac{8D_i}{\pi c_i}$$

$$g_i = \frac{1}{3d_i l_i} [(d_i + l_i)^3 - (d_i^2 + l_i^2)^{1.5}] - d_i$$

The particle resulting from the collision of particles i and j has a diameter d_k given by

$$d_k^3 = d_i^3 + d_j^3$$

Each size category k has an upper bound d_{ku} and lower bound d_{kl} “halfway” (on a logarithmic scale) between the adjacent size categories.

We can calculate the total *loss rate per second* in particles of size k by summing over all size fractions involving collisions with particles of size k :

$$\frac{\Delta N_k(\text{loss})}{\Delta t} = -N_k \sum_{j=1}^{97} K_{kj} N_j \quad [1]$$

subject to the requirement that the particle must grow large enough to exceed the *upper boundary* d_{ku} of the size category k :

$$d_k^3 + d_j^3 > d_{ku}^3$$

For simplicity we assume that all particles before collision have sizes equal to the midpoint of their size category. The size of the resultant particle is calculated and then the particle is reassigned to the midpoint of the category it ends up in for the next calculation one second later. The upper bound of 97 in the summation reflects the fact that the SMPS has 97 size categories equally spaced on a logarithmic scale between 2 nm and 64 nm (64 categories per decade).

The total *gain rate per second* in particles of size k will be equal to the sum of all collisions involving particles of size i and j (both smaller than k) that result in diameters in the *range* of category k :

$$\frac{\Delta N_k(\text{gain})}{\Delta t} = \sum_{j=1}^{k-1} \sum_{i=1}^j K_{ij} N_i N_j \quad [2]$$

subject to the requirement that $d_{kl}^3 < d_i^3 + d_j^3 < d_{ku}^3$

The total change in N_k per unit time will be the sum of the gains and losses (equations [1] and [2]).

Characteristics of Particles Emitted by Kitchen Appliances

Particle sizes, observed concentrations, and emission rates are provided for the gas stove (Tables S1 and S2), electric stove (Table S3) and electric toaster oven (Table S4). Results for the < 10 nm and > 10 nm categories are broken out separately. Although cooking times varied from 3 min to 2 h, by creating categories with identical or only slightly varying cooking times it was considered justifiable to calculate means and standard deviations for the concentrations and emission rates. Emission rates were not calculated for the cases when the SMPS was in the

kitchen, because the concentrations were not spatially homogenous and the open architecture made it unreasonable to determine a volume to use in the calculations.

The evolution of typical size distributions from an electric stovetop coil and an electric toaster oven is shown in Figures S2 and S3. The initial peaks occur at 8.8 nm and 19 nm, growing to 15 nm and 26 nm over the next 45 min and 20 min (eight 2.5-minute scans), respectively. Possibly the heating element in the electric toaster oven is also creating smaller particles but they are being lost to coagulation before they can escape the closed oven.

A marked change in the size distribution was noted for an electric stovetop coil that had not been used for 3 months previously. A large number of particles > 10 nm were produced on the first use following this period, with a much smaller number on the second use and an even smaller number on the third use the next day (Figure S4). Meanwhile the number of small particles < 10 nm produced each time was nearly constant. A possible explanation is burning off dust that collected during the period of disuse.

Model fitting

To reduce complexity and excessive variability in presenting results, the 97 size categories were reduced to 19 for some calculations, with each containing 5 of the original size categories (except for the first combined category, from 2.02 nm to 2.5 nm, which contains 7 original size categories). Each of the new combined categories is represented by the median size.

Examples of coagulation calculations for the gas stove and the electric stove, using the above 19 categories, are shown in Figures S5 and S6. The square markers represent the observed number changes between successive scans 2.5 min apart, corrected by subtracting the effect of the measured air change rates and the theoretical deposition rates. The curve represents the calculated number change due to coagulation, using some particular model. In Figure S5 (the gas stove), the best model was one using a Hamaker constant of 20 kT, whereas in Figure S6 (the electric stove), the best model used a Hamaker constant of 200 kT. This is consistent with the observed larger values for Hamaker constants exhibited by metals compared to hydrocarbons, assuming that the particles from the electric heating elements consist partly or wholly of the metals composing the heating element.

For 62 of the tests, the six models described in the main text were fit to the data and one model was selected as providing the best fit. Table S5 presents the results. For the electric toaster oven, a single model sufficed: the model with a Hamaker constant of 200 kT and no fractal correction. For the electric stovetop coils, although several models provided the best fits to different experiments, the Hamaker constant of 200 kT was also favored over the 20 kT alternative in 19 of 25 experiments, providing further support for the assumption that the particles consist mainly of metals from the heating elements. For the gas burner, on the other hand, the 20 kT alternative was more commonly selected as the best fit (16 of 26 cases), consistent with a composition mainly of hydrocarbons.

Figure captions

Figure S1. Floor plan of NIST research house.

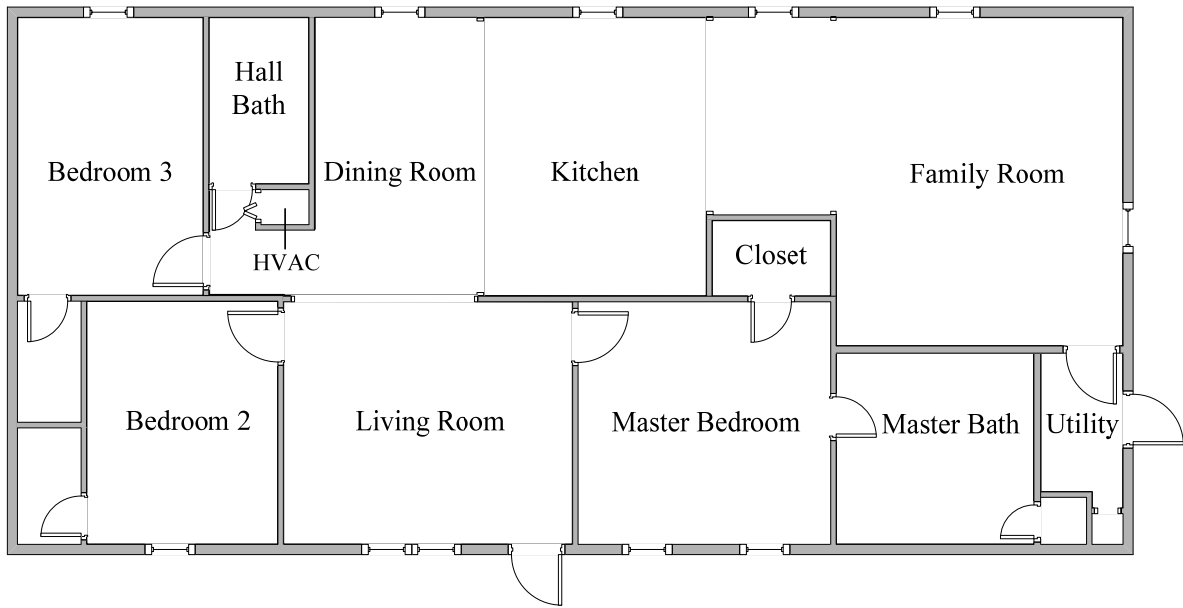
Figure S2. Evolution of size distribution from an electric stovetop coil. Initial peak at 9.8 nm. Error bars are not shown due to the figure complexity but are approximately 12 % for most size categories, and > 12 % for the tails of the distribution.

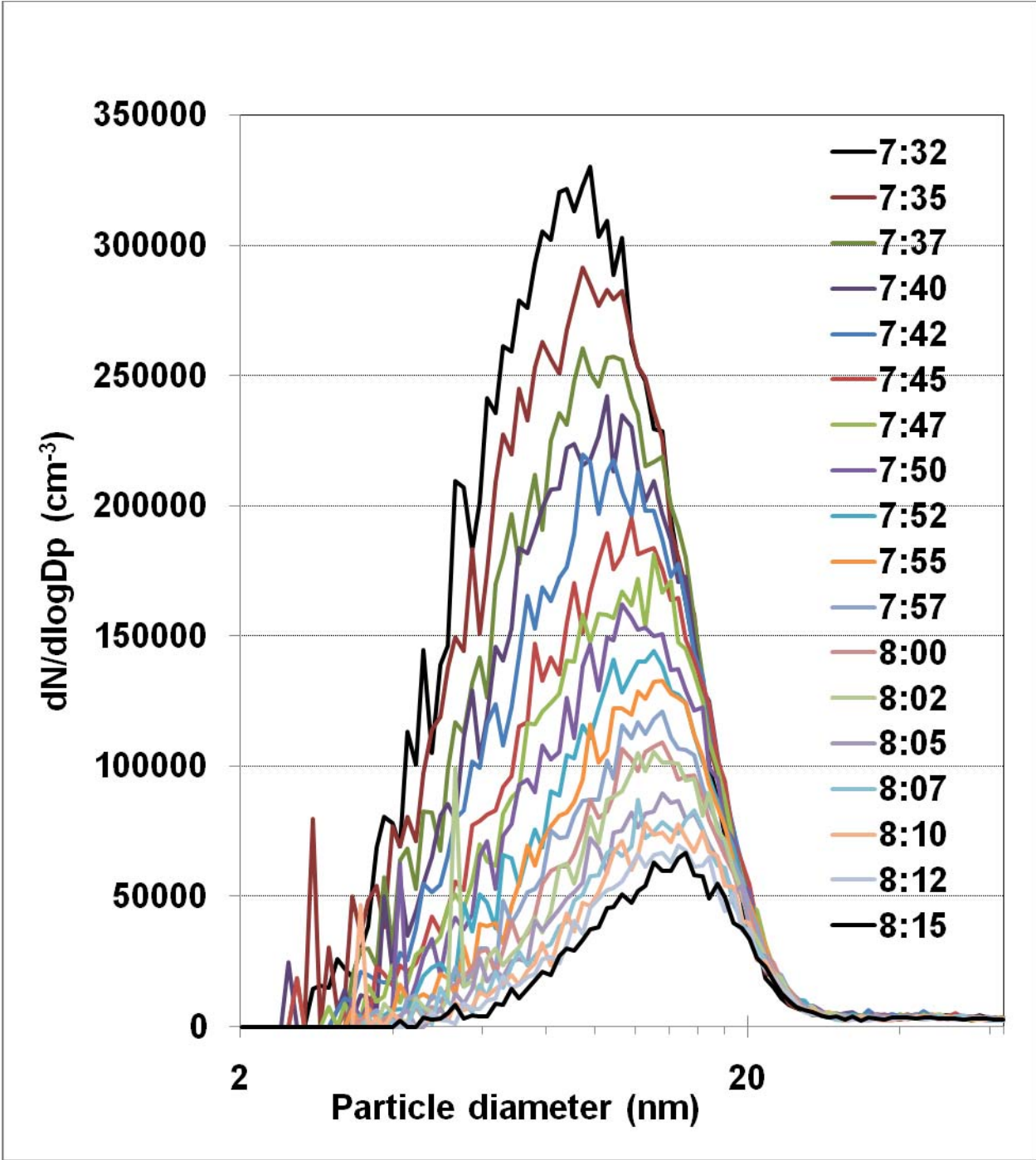
Figure S3. Evolution of size distribution from an electric toaster oven. Initial peak at 18.8 nm. Error bars are not shown due to the figure complexity but are approximately 12 % for most size categories, and > 12 % for the tails of the distribution.

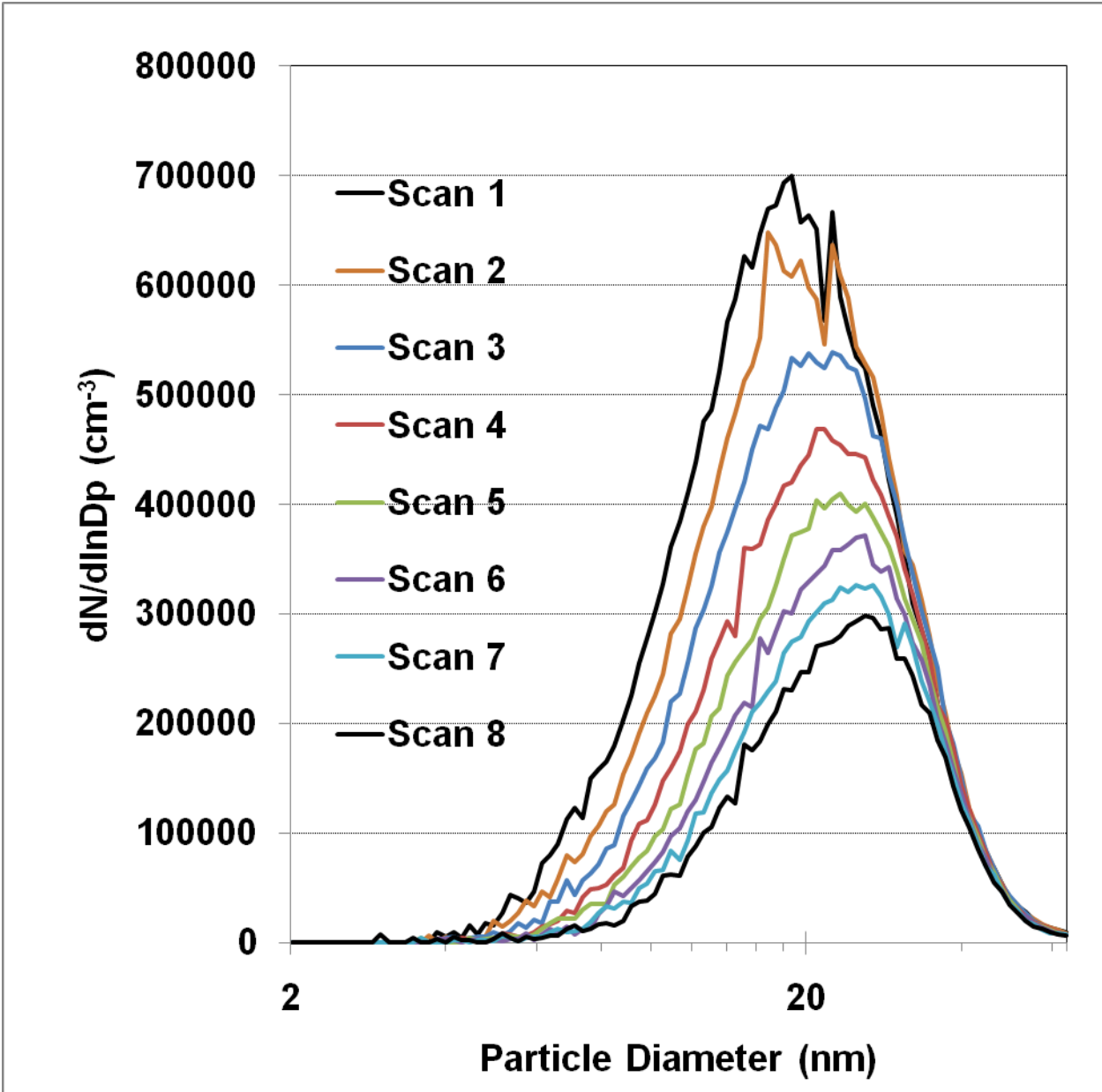
Figure S4. Decrease in numbers of particles > 10 nm with succeeding experiments on an electric stovetop coil. Error bars of about 2 % are not visible on this scale.

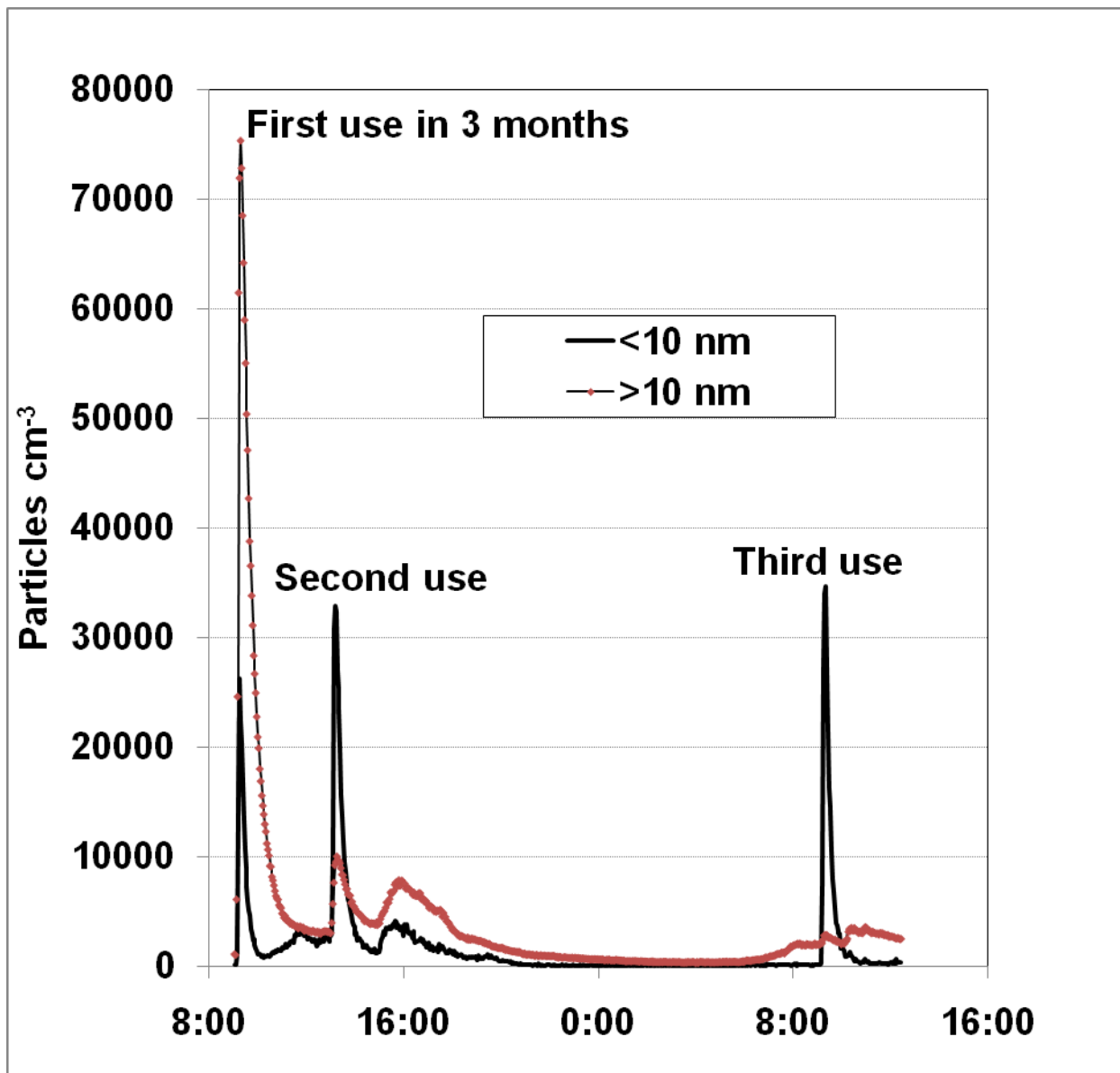
Figure S5. Calculated number concentration changes between successive scans due to coagulation compared to the observed value corrected for measured air change rates and theoretical deposition rates. First scan was that with the highest number concentration following shutoff of the source. Model included a van der Waals/viscosity correction using a Hamaker constant of 20 kT and a fractal dimension of 1.7 for particles > 24 nm. Gas stovetop burner heated for 2 hours on 3/9/07. Error bars for the observed values are about 5 %.

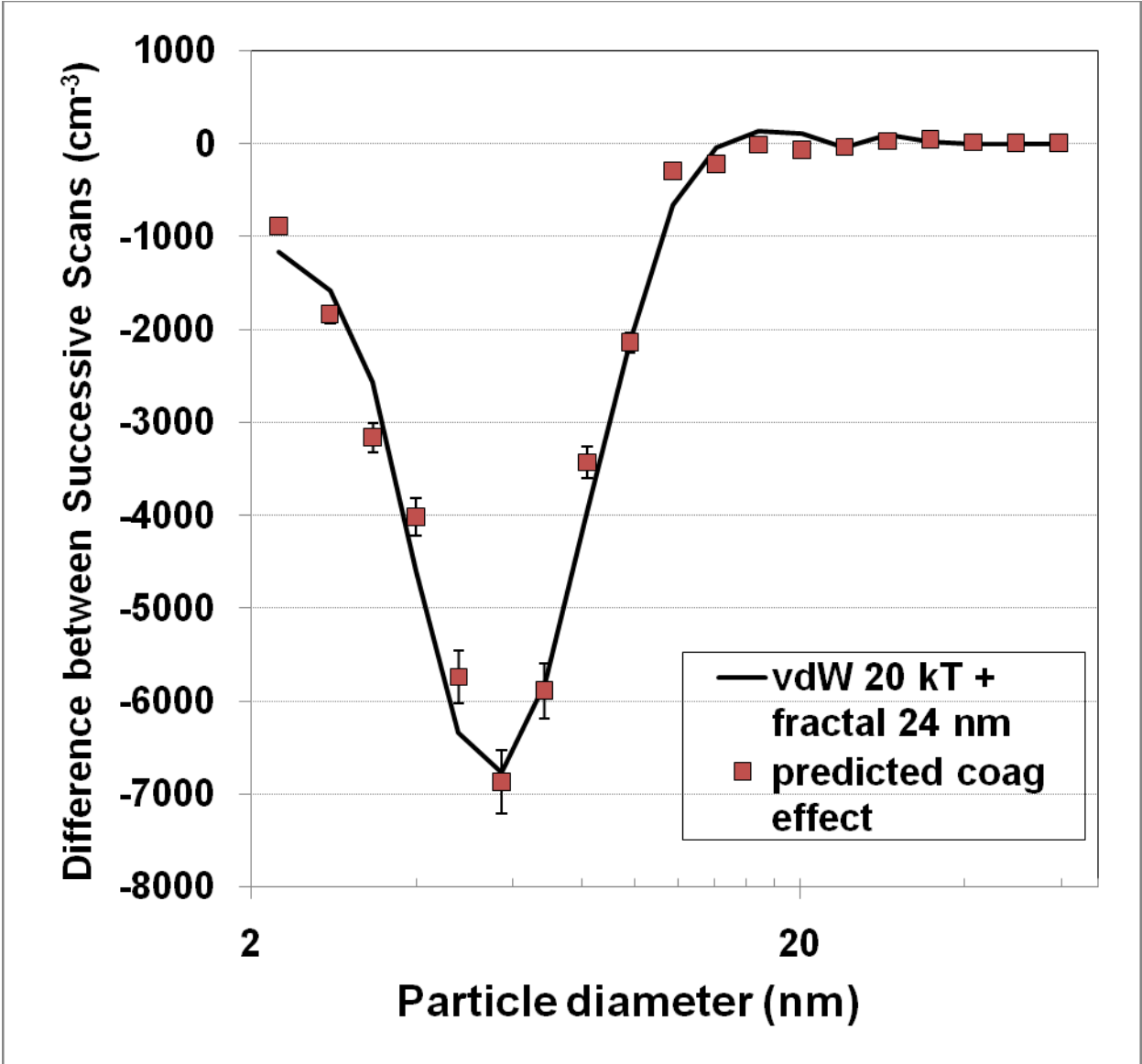
Figure S6. Calculated number concentration changes between successive scans due to coagulation compared to the observed value corrected for measured air change rates and theoretical deposition rates. The first scan was the one following the scan with the highest observed total concentration following shutoff of the source. Model included a van der Waals/viscosity correction using a Hamaker constant of 200 kT and a fractal dimension of 1.7 for particles > 24 nm. Electric stovetop coil heated for 20 min on 5/2/08. Error bars for the observed values are about 5 %.











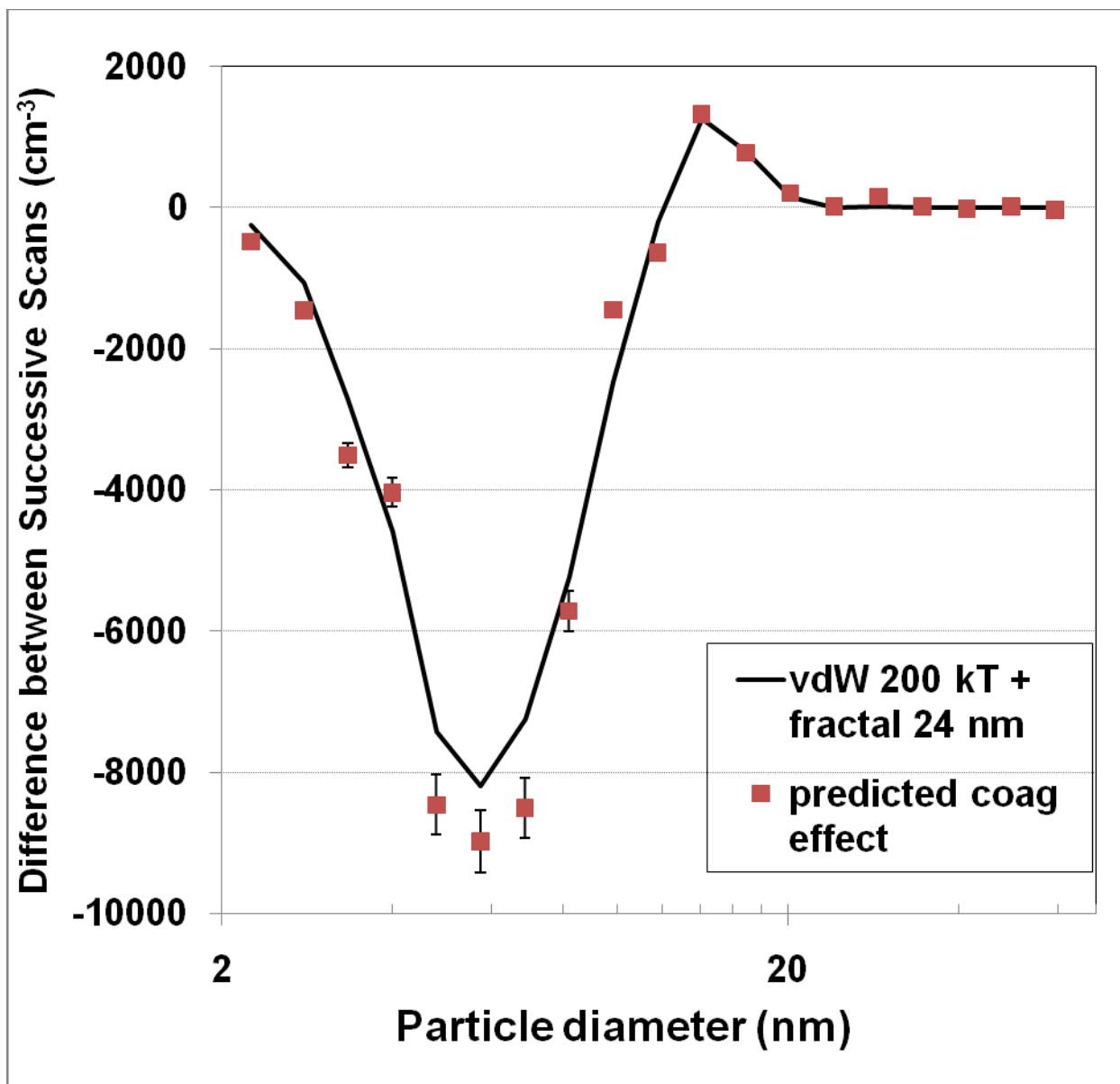


Table S1. Gas stove, no food or water: particle concentrations, emission rates, and size distribution characteristics.

Component	Cook type	No. of Expts	Mean Gas Use (L)	Time (min)	Mean peak concentration ($\times 1000 \text{ cm}^{-3}$)		Mean emission rate ($\times 10^{12} \text{ min}^{-1}$)		Geo. Mean (nm)	Geo. Std. Dev.
					<10 nm	>10 nm	<10 nm	>10 nm		
<i>SMPS in Master Bedroom</i>										
Burner		1	272	64	350	87	1.9	0.5	6.5	1.62
Burner		7	83	17 to 26	584(97) ^b	66(23)	11(2.0)	1.2(0.4)	5.7(0.4)	1.49(0.05)
Burner		12	46	10 to 14	350(144)	12(6.9)	11(4.1)	0.4(0.2)	5.2(0.3)	1.46(0.06)
Burner		3	19	4	82(10)	11(8.8)	7.2(0.9)	1.0(0.8)	6.4(1.2)	1.47(0.04)
Oven	Bake	2		50	58(45)	22(16)	0.4(0.3)	0.2(0.1)	8.3(3.5)	1.98(0.11)
Oven	Bake	4		20 to 23	42(23)	140(130)	0.7(0.3)	2.4(2.3)	14.4(7.1)	1.81(0.13)
Oven	Bake	2		11	72(39)	40(49)	2.3(1.2)	1.3(1.6)	9.4(7.2)	1.81(0.32)
Broiler	Broil	6		16 to 23	110(97)	200(160)	1.9(1.6)	3.4(2.6)	15.1(7.3)	1.78(0.11)
<i>SMPS in kitchen</i>										
Burners (4)		1	1007	63	1500	720	N/A	N/A	7.0	1.63
Burner		3	495	111 to 119	1500(152)	150(58)	N/A	N/A	4.4(0.4)	1.64(0.09)
Burner		1	130	31	425	37	N/A	N/A	6.5	1.36
Burner		3	18	4	550(230)	38(62)	N/A	N/A	6.2(2.3)	1.44(0.14)
^a N/A SMPS in kitchen; too close to source to calculate an emission rate										
^b Standard deviations in parentheses										

Table S2. Cooking with food or water on gas stove: particle concentrations, emission rates, and size distribution characteristics.

Component	Cook type	Food type	Pot type	No. of Expts	Time (min)	Gas use (L)	Peak concentration ($\times 1000 \text{ cm}^{-3}$)		Emission rate ($\times 10^{12} \text{ min}^{-1}$)		Geo. Mean (nm)	Geo. Std. Dev.
							<10 nm	>10 nm	<10 nm	>10 nm		
<i>SMPS in Master Bedroom</i>												
Burner	Boil	Water (1 L)	Saucepan	3	11	48	140(28) ^b	24(13)	4.9(1.0)	0.8(0.4)	6.6 (0.9)	1.48(0.22)
Burner	Boil	Water (700 mL)	Saucepan	5	7	27	140(3.5))	18(4.8)	6.9(0.2)	1.0(0.5)	6.2(0.6)	1.53(0.20)
Burner	Boil	Water (350 mL)	Saucepan	3	4	17	80	23(4.7)	7.0(0.0)	1.9(0.3)	6.3(1.1)	1.72(0.22)
Burner	Simmer	Rice	Saucepan	2	28	35	100	28(17)	1.4	0.4(0.3)	8.5	1.65(0.14)
Burner	Simmer	Reheating	Saucepan	2	6	8	21	12(13)	0.9	1.3(1.6)	5.5	1.82(0.05)
Burner	Stir-fry	oil, broccoli	Wok	4	4	13	13	52(17)	1.1	5.2(0.9)	17	1.79(0.10)
Burner	Fry	Eggs	Frying pan	2	6	13	10	58(39)	0.9	4.5(4.2)	20	1.71(0.10)
Burner	Fry	Bacon	Frying pan	2	14	23	18	58(18)	0.4	1.5(0.2)	16	1.78(0.02)
Oven	Bake (175 °C)	Rice (reheated)	Ceramic	2	15	73	19	44(58)	0.5	1.0(1.3)	12(10)	1.88(0.02)
Oven	Bake (250 °C)	Baked potato	Oven rack	2	42	226	47	141(69)	0.4	1.2(0.4)	13	1.81(0.06)
Broiler	Broil	English muffin	Broiler rack	4	7	56	16(8.5)	46(37)	1.0(0.1)	3.3(3.7)	13(4.1)	1.66(0.18)
<i>SMPS in kitchen</i>												
Burner	Boil	Water (350 mL)	Saucepan	3	6	26	520(140)	250(63)	N/A ^a	N/A	8.8(0.1)	1.53(0.08)
Burner & broiler	Fry & toast	Bacon, eggs, & muffin	Frying pan	2	11	56	90(28)	210(110)	N/A	N/A	13(0.4)	1.74(0.02)
^a N/A -- Emission rate not calculated because SMPS too close to source												
^b Standard deviations in parentheses												

Table S3. Electric stove: Particle concentrations, emission rates, and size distribution characteristics

	No. of Expts	Pot type	Food type	Cook type	Amount (mL)	Time (min)	Peak concentration ($\times 1000 \text{ cm}^{-3}$)		Emission rate ($\times 10^{12} \text{ min}^{-1}$)		Geo. Mean (nm)	Geo. Std. Dev.
							<10 nm	>10 nm	<10 nm	>10 nm		
Stovetop (no food)												
	20	None	None	Heat		4	45(24) ^a	29(41)	4.0(2.1)	2.5(3.5)	7.5(2.5)	1.60(0.15)
	10	None	None	Heat		20-38	180(90)	76(65)	3.2(1.6)	1.1(0.9)	5.9(2.1)	1.67(0.27)
Stovetop (food or water)												
	3	Saucepan	Water	Boil	350	5	20(4.2)	12(13)	1.4(0.3)	0.8(0.9)	8.2(2.9)	1.74(0.03)
	3	Saucepan	Water	Boil	1000	11	44(1.2)	9.0(11)	1.5(0.04)	0.3(0.4)	6.6(1.7)	1.56(0.10)
	5	Saucepan	Water,potatoes	Boil	1000	30	55(35)	89(81)	0.6(0.4)	1.0(0.9)	12(3.4)	1.60(0.10)
	3	Saucepan	Rice	Boil/simmer	200	30	5.4(3.9)	26(21)	0.1(0.04)	0.3(0.2)	15(8.7)	1.69(0.17)
	2	Frying pan	Peanut oil	Saute	30	3	3.4(0.5)	46(12)	0.4(0.1)	5.9(1.6)	25(2.1)	1.78(0.05)
	1	Frying pan	Bacon, eggs	Fry	3 strips bacon	15	5	47	0.1	1.1	24	1.88
Oven (empty)												
	7	None	None	Bake (230 °C)		20	2.4(0.5)	12(15)	0.04(0.01)	0.2(0.3)	18.1(7.2)	1.98(0.25)
	5	None	None	Broil		20	4.1(1.0)	9.0(8.8)	0.07(0.02)	0.2(0.2)	10.4(4.7)	2.19(0.44)

^a Standard deviations in parentheses

Table S4. Electric toaster oven: particle concentrations, emission rates, and size distribution characteristics.

	Food type	Cook type	Oven temp (° C)	Time (min)	Peak concentration (cm ⁻³)		Emission rate (× 10 ¹² min ⁻¹)		Geo. Mean (nm)	Geo. Std. Dev.
					<10 nm	>10 nm	<10 nm	>10 nm		
<i>Empty, SMPS and oven in MBR, door closed</i>					<10 nm	>10 nm	<10 nm	>10 nm		
	None	Toast		6	24000	720000	0.2	6.0	28	2.20
	None	Toast		12	130000	1400000	0.5	5.8	30	1.61
	None	Bake	230	20	50000	1200000	0.1	3.0	32	1.54
	None	Bake	230	20	115000	1200000	0.3	3.0	28	1.62
<i>Empty, oven in kitchen, SMPS in MBR</i>										
	None	Bake	230	20	45000	260000	0.8	4.6	17	1.64
	None	Bake	230	20	45000	210000	0.8	3.7	16	1.63
	None	Bake	230	20	44000	190000	0.8	3.3	16	1.63
	None	Bake	230	20	1500	210000	0.03	3.7	35	1.69
	None	Broil		20	40000	220000	0.7	3.9	17	1.62
	None	Broil		20	40000	300000	0.7	5.3	18	1.58
	None	Broil		20	4500	130000	0.1	2.3	24	1.57
<i>Food</i>										
	English muffin	Toast		12	2000	86000	0.1	2.5	28	1.60
	English muffin	Toast		11	4000	52000	0.1	1.7	22	1.70
	Bread	Toast		6	100	31000	0.01	1.8	49	1.64
	Potato	Bake	230	20	6800	140000	0.1	2.5	22	1.57

Table S5. Best Fits of Coagulation Models to Different Stove and Cooking Types

<i>Appliance/Component/Cooktype</i>	Number of Experiments Best Fit by the Indicated Correction Factor					
	<i>vdW 20</i>	<i>vdW 200</i>	<i>vdW 20 + fractal 24</i>	<i>vdW 200 + fractal 24</i>	<i>vdW 20 + fractal</i>	<i>vdW 200 + fractal</i>
Gas stovetop burner--no food or water	3	9	9		1	
Gas stovetop burner--boiling water		1			2	1
Gas oven--no food or water						3
Electric stovetop coil--no food or water		4	4	5		
Electric stovetop coil--boiling water	1	1	1	5		4
Electric toaster oven--no food or water		7				
Electric toaster oven--baked potato		1				
<i>Notes:</i>						
vdW 20 -- Van der Waals/viscosity correction with the Hamaker constant set to 20 kT						
vdW 200 -- Van der Waals/viscosity correction with the Hamaker constant set to 200 kT						
fractal -- All particles assumed to follow fractal dimension of 1.7						
fractal 24 -- Only particles > 24 nm assumed to follow fractal dimension of 1.7						